11.4
INVITED

THE EFFECT OF ELECTRON BEAM INDUCED SPACE CHARGE ON SPARK GAP BREAKDOWN *

Y.H. Tzeng, E.E. Kunhardt, and M. Kristiansen
Department of Electrical Engineering
Texas Tech University
Lubbock, Texas 79409 USA

A.H. Guenther
Air Force Weapons Laboratory
Kirtland Air Force Base, New Mexico, 87117, USA

Abstract

An investigation into the effect of electron beam induced space charge on the insulating property of a gas in a spark gap is presented. The characteristics of the gas transition from insulator to conductor show strong dependence on the amount and location of the space charge introduced. Investigations of the delay time and the characteristics of the conducting channel have been made. The delay time from the injection of the e-beam to the collapse of the gap voltage ranges from 10^{-9} to 10^{-3} second. From open shutter photography, we observe that the character of the conducting channel is quite varied. Dark, diffuse, filamentary, or diffuse followed by filamentary (single or multiple) channels have been observed, depending on the space charge conditions. The fundamental processes leading to the collapse of the insulating property of the gas for various experimental conditions are discussed.

I. Introduction

The development of high power switches has recently received a great deal of attention as a common and crucial area of interest for scientists working on high power laser, fusion, high current charged-particle accelerators, and weapons-effect simulators. These switches must be capable of fast and repetitive transfer or interruption of high voltage, high current from an energy storage device to various transducers. To meet these requirements a number of novel switches have been proposed.[1] In many of these approaches, switching is accomplished by causing a transition between insulating and conducting states of a gas. The various devices that operate in this fashion differ mainly in the way this transition is initiated and in the characteristics of the conducting stage, i.e. whether it be a diffuse or filamentary discharge.

The electron beam has been shown to be a powerful tool for initiating either a self-sustaining or a nonself-sustaining discharge in a high pressure gas in a spark gap.[2,3] This paper presents an investigation into the effects of the space charge induced by an electron-beam on spark gap operation. These effects are fundamental to the understanding of the e-beam switching.

In Section II of this paper, the experimental setup and procedures are described. In Section III, the results are presented. These results significantly extend those presented in a previous paper.[4] We give further discussions of the physical processes occurring in e-beam switching. Recommedations for e-beam switching applications are given in Section IV.

II. Experimental Arrangement

A diagram of the apparatus used for these investigations is shown in Fig. 1. This setup has been described in detail in references 4 and 5. Briefly, the experiment consists of an energy storage element, a gas insulated, pressurized spark gap, and a source of energetic electrons. The energy storage element and the spark gap are contained within the high pressure vessel of a Van de Graaff charged coaxial line. The line can be charged to approximately 1 MV and delivers a rectangular pulse of approximately 10 ns, full width at half maximum duration. The electron beam is generated by a cold cathode field emission vacuum diode which is located behind the electrode facing the Van de Graaff charged line. Modification to the diode described in reference 4 are discussed in reference 5. A better characterization of the e-beam has also been made (see reference 5).

The effects that we have studied include: (1) The characteristics of the resulting current pulse (i.e. amplitude, length, risetime, and waveform); (2) The switch delay time and jitter; and (3) The spatial character of the discharge channel.

The parameters varied during the course of these investigations are: (1) The gap polarity (depending on how the Van de Graff is charged, the target electrode can be either positive or negative); (2) The gap voltage V_g (varied between 30 percent and 95 percent of the selfbreakdown voltage, which ranges from 40 kV to 500 kV); (3) The gas pressure (3-7 atm); (4) The type of gas (N_2, and mixtures of N_2 and SF_6); (5) The e-beam current (varied by putting a 1 mm thick aluminum mask with the desired area of uniformly distributed holes in front of the beam. The current can be varied from about 4 A to 1 kA); (6) The average e-beam energy (35 keV to 180 keV); (7) The e-beam pulse length (2-50 ns).

III. Results and Discussions

Since the parameter space investigated is large, we have chosen the type of gas and the gap voltage polarity, in reference to the direction of the electron beam, to subdivide this space. This choice is based on the similarities of the physical processes that occur in the regimes defined by these parameters. We shall first present the results obtained using pure nitrogen, followed by those obtained with mixtures of N_2 and SF_6.

*Supported by AFOSR and ARO

Report Documentation Page

Form Approved
OMB No. 0704-0188

1. REPORT DATE	2. REPORT TYPE	3. DATES COVERED
JUN 1981	**N/A**	**-**

4. TITLE AND SUBTITLE	5a. CONTRACT NUMBER
The Effect Of Electron Beam Induced Space Charge On Spark Gap Breakdown	5b. GRANT NUMBER
	5c. PROGRAM ELEMENT NUMBER
6. AUTHOR(S)	5d. PROJECT NUMBER
	5e. TASK NUMBER
	5f. WORK UNIT NUMBER
7. PERFORMING ORGANIZATION NAME(S) AND ADDRESS(ES) **Department of Electrical Engineering Texas Tech University Lubbock, Texas 79409 USA**	8. PERFORMING ORGANIZATION REPORT NUMBER
9. SPONSORING/MONITORING AGENCY NAME(S) AND ADDRESS(ES)	10. SPONSOR/MONITOR'S ACRONYM(S)
	11. SPONSOR/MONITOR'S REPORT NUMBER(S)

12. DISTRIBUTION/AVAILABILITY STATEMENT
Approved for public release, distribution unlimited

13. SUPPLEMENTARY NOTES
See also ADM002371. 2013 IEEE Pulsed Power Conference, Digest of Technical Papers 1976-2013, and Abstracts of the 2013 IEEE International Conference on Plasma Science. Held in San Francisco, CA on 16-21 June 2013. U.S. Government or Federal Purpose Rights License.

14. ABSTRACT
An investigation into the effect of electron beam induced space charge on the insulating property of a gas in a spark gap is presented. The characteristics of the gas transition from insulator to conductor show strong dependence on the amount and location of the space charge introduced. Investigations of the delay time and the characteristics of the conducting channel have been made. The delay time from the injection of the e-beam to the collapse of the gap voltage ranges -9 -3 from 10 to 10 second. From open shutter photography, we observe that the character of the conducting channel is quite varied. Dark, diffuse, filamentary, or diffuse followed by filamentary (single or multiple) channels have been observed, depending on the space charge conditions. The fundamental processes leading to the collapse of the insulating property of the gas for various experimental conditions are discussed.

15. SUBJECT TERMS

16. SECURITY CLASSIFICATION OF:			17. LIMITATION OF ABSTRACT	18. NUMBER OF PAGES	19a. NAME OF RESPONSIBLE PERSON
a. REPORT	b. ABSTRACT	c. THIS PAGE			
unclassified	**unclassified**	**unclassified**	**SAR**	**7**	

Because SF_6 is electronegative, the nature of the electron beam induced space charge is significantly different from that for pure N_2. This has a great influence on the subsequent evolution of the space charge in the gap, and ultimately on the characteristics of the pulse observed at the load.

In general, for pure N_2 and negative gap voltage polarity (i.e. the electron beam is retarded by the external field), the discharge current characteristics and the conducting channel luminosity are strong functions of e-beam current amplitude and pulse length, and are relatively weak functions of average e-beam energy. This is also observed for positive gap polarity. Figure 2 shows the discharge current pulses at the load as a function of e-beam current amplitude, and pulse length for both gap voltage polarities. For both gap voltage polarities, no filamentary arc channels are observed when the amount of space charge introduced by the e-beam is large. All the e-beam initiated discharge current pulses shown in Fig. 2 correspond to diffuse discharge channels. Since the discharge current source is a charged transmission line with a two-way delay time of 10 ns and the load is matched to the line, the discharge current pulse is a square pulse with a duration of 10 ns only when the gap resistance is small compared to the characteristic impedance of the charged transmission line (50 ohm in this experiment). When the gap resistance is high, the mismatching created will cause reflections, thus forming a current pulse longer than 10 ns with a smaller amplitude. Thus, from Fig. 2, we note that for the same average e-beam energy the discharge current pulse gets smaller in amplitude, has longer risetime and becomes wider as the e-beam current is lowered or made shorter in duration. This implies that the gap resistance decreases when the e-beam current increases. Using the same arguments, we find that when the target electrode is charged negative and the gas pressure is increased from 5 atm to 7 atm, the gap resistance increases considerably. The variation of gap resistance due to a similar pressure change for the positive target case is not observed. A 700 A, 60 keV, 35 ns electron beam is used for both of these gas pressure experiments. The discharge current pulse risetime was observed to range from 2.5 ns to more than 10 ns. The lower limit is the same as that for a selfbreakdown pulse. In general, the smaller the e-beam current is, the longer the risetime is. From this kind of measurements we conclude that the delay time measured from the injection of the e-beam to the appearance of a sharp rise in the discharge current is less than 1 ns (not including the delay time of the transmission line used for diagnostics). Similarly, the jitter is lower than the resolution of the experimental set-up (sub-nanosecond). In general, the variation of delay time with respect to gap voltage polarity, gap voltage, gas pressure, e-beam energy and current is not detectable. A superposition of five discharge current pulses is shown in Fig. 3.

The spatial characteristics of the e-beam initiated discharge channel is determined from open shutter photographs. Examples are shown in Fig. 4 for a positive target electrode and in Fig. 5 for a negative target electrode. For the same polarity, the conducting channel luminosity varied as we changed the experimental conditions (e.g. e-beam current amplitude, e-beam pulse length, e-beam cross section, number of e-beams, gap voltage, etc). The light distribution in the gap changes with polarity, indicating that there are different processes leading to the discharges. In general, the discharge channel is broad except when the amount of space charge induced by the beam is small. In this case, the discharge channels are filamentary (single or multiple), and large delays are observed (hundreds of ns) Figure 6 is an illustration of this condition. In this case a 4 A, 150 keV, 10 ns e-beam has been used to trigger a spark gap pressurized to 3 atm of N_2. The gap voltage is close to selfbreakdown voltage (i.e. 95 % V_{sb}). Multichannel discharges have also been achieved using multiple electron beams. Up to eight channels have been simultaneously created (see Fig. 4a).

The various results discussed in the above paragraphs may be explained as follows. When the e-beam is injected into the gap towards a negatively charged electrode, it is retarded by both the gas and the electric field. The spatial distribution of the induced space charge is thus determined by the beam energy, the gas pressure and the magnitude of the applied field. The distribution and amount of the induced space charge together with the gap conditions, determine the properties of the discharge channels and current characteristics. Simple calculation shows that the current generated in the external circuit due to the motion of the space charge induced by a 1 ns, 500 A, 60 keV e-beam injected into a gap charged to 150 kV in 3 atm N_2 is on the order of kA. This explains the short delay times observed (ns). Once the e-beam is injected into the gap, the ionized and excited gas molecules will emit photons in a short period of time. Those photons having low absorption cross section may reach the cathode. If their energy is higher than the work function of the electrode material, they can release electrons via the photoelectric effect. This constitutes a supply of electrons distributed over a large area of the cathode. In their way to the anode the photoelectrons form a number of avalanches. Since the avalanches are overlapping, the space charge enhanced field is uniform, and therefore, we see a broad discharge channel. This phenomenon is similar to that observed by Koppitz.[6] The avalanches evolve until the ion space charge resulting from the e-beam induced plasma is neutralized. This is seen in Fig. 5. If this space charge is small (for low e-beam current, for example) multiple avalanches will develop, resulting in a filamentary discharge as shown in Fig. 6. When the target electrode is charged positive, the injected fast electrons can penetrate across the gap and create a conducting channel by ionizing the gas molecules. The conductivity of the channel depends on the amount of space charge introduced. The properties of this discharge are similar to the e-beam sustained discharge discussed in reference 3. This experiment shows the fast turn-on of this mode of operation and its capability of delivering a 0.5 kA/cm^2 discharge current density.

When mixtures of N_2 and SF_6 are used as the gas medium, the character of the discharge is different than when pure N_2 is used. In general, when the gap voltage is higher than some threshold voltage, V_t (Fig. 7a), the discharge channel is filamentary (single or multiple) with a discharge current pulse similar to the selfbreakdown pulse. The threshold voltage, V_t, for the onset of this filamentary discharge depends on gas pressure, % SF_6, e-beam conditions, etc. When the gap voltage is lower than this threshold, no filamentary arc channel is observed. The discharge current amplitude is then very small compared to that of selfbreakdown. After the discharge stops the voltage of the charged line drops to only a fraction of its original voltage. These phenomena are observed for both gap voltage polarities.

The delay time, from the injection of e-beam to the detection of the discharge current pulse at the load, not including the delay time due to the transmission line for diagnostics, has been measured and is shown in Fig. 7 for negative target electrode and in Fig. 8 for positive target electrode. For the case of negative target electrode, the e-beam energy plays an important role in determining the delay time. From Fig. 7b, we note that for a ten fold increase in e-beam current, the delay time decreases by 70 %. Moreover, from Fig. 7c, we note that the delay time increases by 500 times when the average e-beam energy decreases to 60 % and the e-beam current decreases to 33 %. Therefore, we conclude that the delay time is a strong function of the average e-beam energy and a relatively weak function of the e-beam current. For the case of a positive target electrode, both e-beam current and average energy show important effects on the delay time. This is shown in Fig. 8a, 8b, and 8e. In Fig. 7d and 8f, the dependence of the delay time on the gas pressure is displayed. The delay time increases with increasing gas pressure for the case of a negative target electrode, while it decreases with increasing gas pressure for the case of a positive target electrode. The dependence of the delay time on the ratio of mixtures of N_2 and SF_6 is displayed in Fig. 7e and 8d.

These observations can be explained as follows. The attachment coefficient of SF_6 is high for low energy electrons and increases with decreasing ratio of electric field to gas pressure. Therefore, most of the low energy electrons produced in the gap will attach to SF_6 to form negative ions. Since the drift velocity of these ions is low, the space charge current induced in the external circuit right after the injection of the e-beam is small. When the target electrode is negative, the ionized gas close to the anode virtually extends the anode and enhances the electric field due to asymmetry and reduction of the cathode-virtual-anode distance. Since the net ionization coefficient, (the difference between ionization and attachment) is a strong function of the ratio of electric field to gas pressure, the electron number density close to the symmetrical axis of the electrodes grows faster than those at other places. When the injected e-beam has higher energy, it can penetrate farther. The electric field in the cathode-virtual-anode region determines the further development of the breakdown. Under some conditions, a filamentary arc channel may develop. Therefore, the delay time is strongly dependent on the e-beam penetration depth, which is a function of e-beam energy, gap voltage and gas pressure. When the target electrode is positive, the inhomogeneous ionization of the gas by the non-monoenergetic electron beam and the resulting nonuniform distribution of space charge are thought to be the reasons leading to the breakdown of the spark gap. When the gap voltage is lower than the threshold, V_t, the space charge enhanced electric field is not strong enough for the spark gap to break down. A diffuse discharge channel, which ceases before the charged line voltage drops to zero, is observed under this condition.

IV. Conclusions

The fundamental processes leading to the collapse of the insulating property of the gas for the various experimental conditions studied have been elucidated. It has been shown that with e-beam triggering, diffuse or multichannel discharges can be achieved. For high power switching applications, the diffuse discharge channel obtained under certain conditions provides the beneficial characteristics of nonmeasurable delay and jitter, low electrode erosion, fast recovery (because it can be operated at low % V_{sb} and the gas is not fully ionized), and low switch inductance. Moreover, multichannel discharge operation, shown possible with e-beam triggering, provides low gap resistance, low switch inductance, and low electrode erosion compared to that of a single discharge channel.

The ability to tailor the space charge induced by the e-beam to virtually create any type of discharge channel would make this scheme most desirable for spark gap operation. However, the requirements for the e-beam parameters may limit the range of applicability. These requirements have been discussed in Section III.

References

1. T.R. Burkes, M.O. Hagler, M. Kristiansen, J.P. Craig, W.M. Portnoy, E.E. Kunhardt, " A Critical Analysis and Assessment of High Power Switches," Report NP30 Submitted to Naval Weapons Center, Dahlgren, Virginia (1978).

2. A.S. El'chaninov, V.G. Emel'yanov, B.M. Koval'chuck, G.A. Mesyats, and Yu F. Potalitsyn, " Nanosecond-range Triggering of Megavolt Switches," Sov. Phys. Tech. Phys, Vol. 20, No.1. pp 51-54, July 1975.

3. R.O. Hunter, " Electron Beam Controled Switching," Proc. First IEEE International Pulse Power Conference, paper IC8-1, Nov. 1976, Lubbock, Texas.

4. K.McDonald, M. Newton, E.E. Kunhardt, M. Kristiansen, and A.H. Guenther," An Electron-beam Triggered Spark Gap", IEEE Trans. Plasma Science PS8, 181,1980.

5. Y. Tzeng," The Effect of Space Charge Induced by an Electron Beam on Spark Gap Operation", Master Thesis, Texas Tech University, August 1981.

6. J. Koppitz," Nitrogen Discharges of Large Cross Section at High Overvoltage in a Homogeneous Field", J. Phys. D: Appl. Phys 6, 1494 (1973).

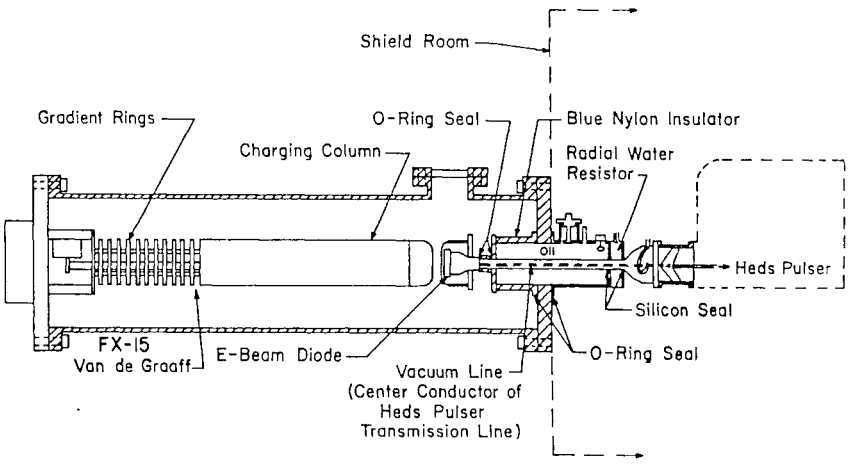

Fig. 1. Experimental Setup.

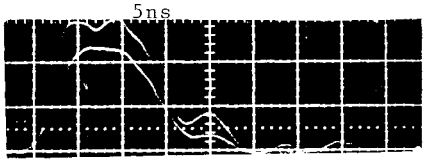

(a) Selfbreakdown (Larger Amplitude, V_{sb}=176kV) E-beam Initiated (Smaller Amplitude, V_g= 132 kV; E-beam: 700 A, 60 keV, 40 ns).

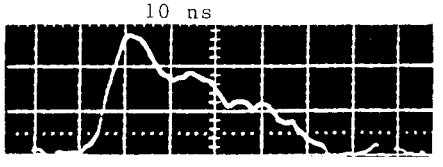

(b) E-beam Initiated (V_g= 132 kV, E-beam: 70 A, 60 keV, 40 ns).

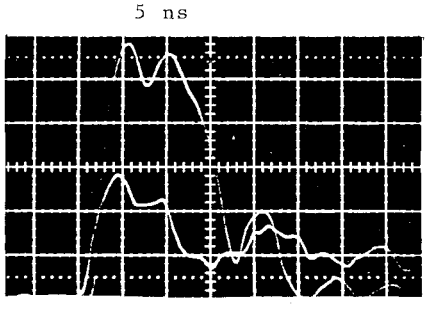

(c) Selfbreakdown (Larger Amplitude, V_{sb}=170kV) E-beam Initiated (Smaller Amplitude, V_g=140 kV; E-beam: 580 A, 70 keV, 2.5 ns).

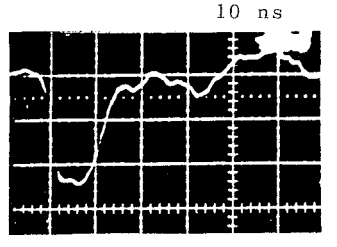

(d) E-beam Initiated Discharge Current Pulse with E-beam Current of 700 A and Average E-beam Energy of 60 keV.

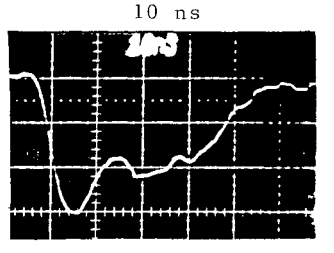

(e) E-beam Initiated Discharge Current Pulse with E-beam Current of 70 A and Average E-beam Energy of 60 keV.

Fig. 2. Discharge Current Pulses.

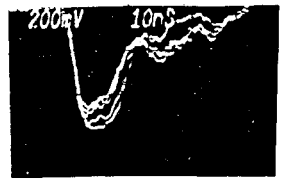

Fig. 3. The Delay and Jitter Measurements.

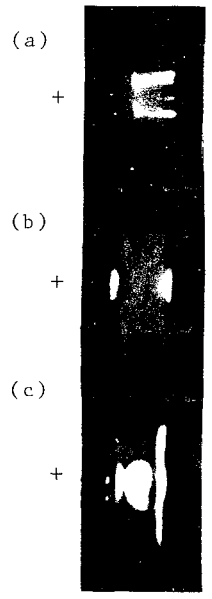

Discharge Channels Initiated by a 4 A, 150 keV, 10 ns E-beam. (A 1 mm Thick Al Mask with 8 Holes was Put in front of the E-beam, and the Gap Voltage was below 95 % V_{sb}.)

Discharge Channel Initiated by a 500 A, 35 keV, 10 ns E-beam.

Discharge Channel Initiated by a 500 A, 35 keV, 2.5 ns E-beam.

Fig. 4. Discharge Channels when E-beam was Injected from Cathode.

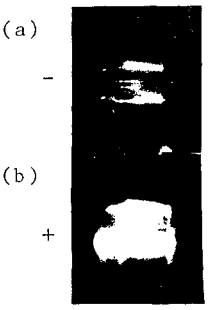

Fig. 6. Discharge Channels Initiated by a 4 A, 150 keV, 10 ns E-beam. (A 1 mm Thick Al Mask with 8 Holes was Put in front of the E-beam.)

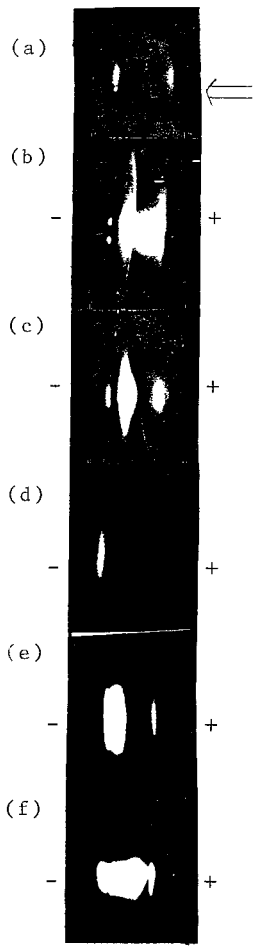

E-beam only

Discharge Channels Initiated by Two E-beams.

Discharge Channel Initiated by a 500 A, 10 ns, 35 keV E-beam.

Discharge Channel Initiated by a 440 A, 60 keV, 3 ns E-beam. (V_g= 72 kV, V_{sb}= 160 kV).

Discharge Channel Initiated by a 440 A, 60 keV, 3 ns E-beam. (V_g=126 kV, V_{sb}= 160 kV).

Discharge Channel Initiated by a 192 A, 35 keV, 3 ns E-beam. (V_g= 156 kV, V_{sb}= 160 kV).

Fig. 5. Discharge Channels when E-beam was Injected from the Anode.

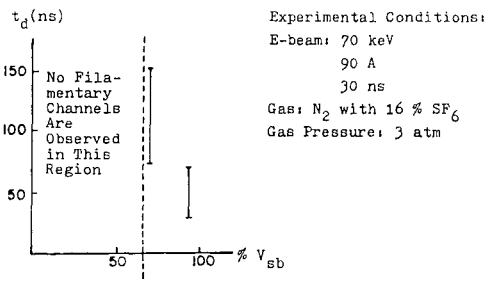

Fig. 7 a. Delay Time vs % V_{sb}.

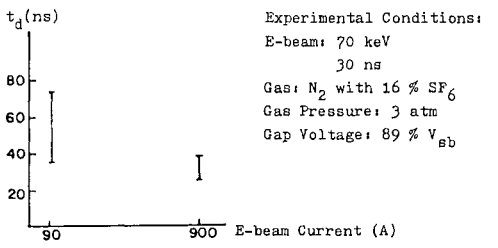

Fig. 7 b. Delay Time vs E-beam Current.

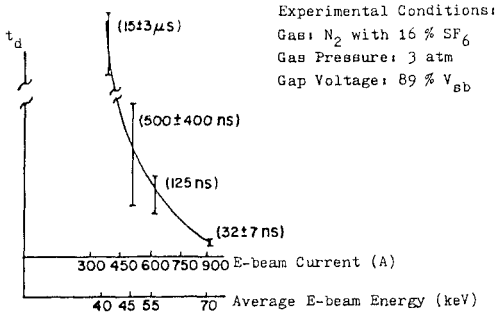

Fig. 7c. Delay Time vs E-beam Current And Energy.

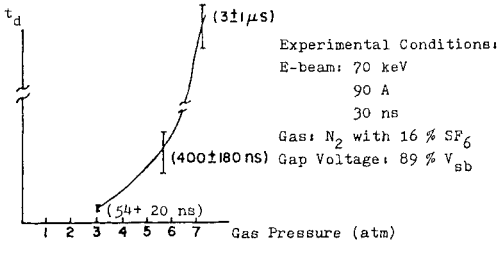

Fig. 7d. Delay Time vs Gas Pressure.

Experimental Conditions:
E-beam: 70 keV
90 A
30 ns
Gas: N_2 with SF_6
Gas Pressure: 3 atm
Gap Voltage: 89 % V_{sb}

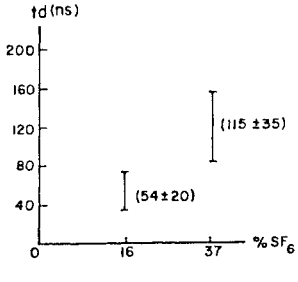

Fig. 7e. Delay Time vs % SF_6

Fig. 7. Delay Time vs E-beam and Gap Conditions.

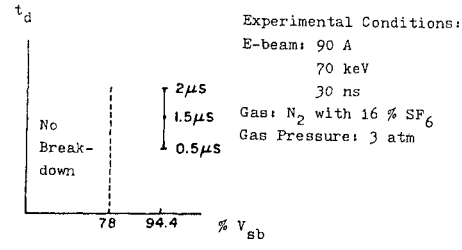

Fig. 8a. Delay Time vs % V_{sb}

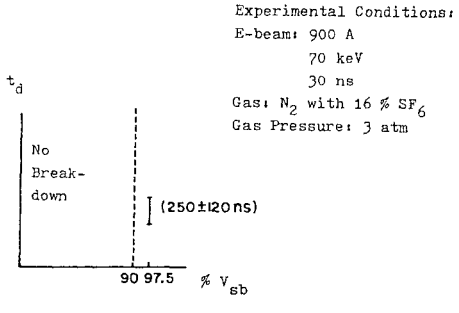

Fig. 8b. Delay Time vs % V_{sb}

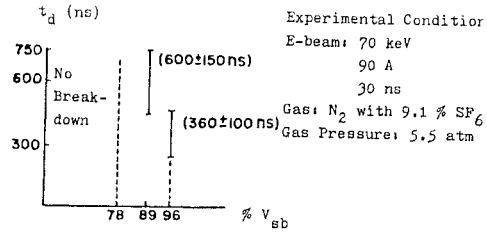

Fig. 8c. Delay Time vs % V_{sb}

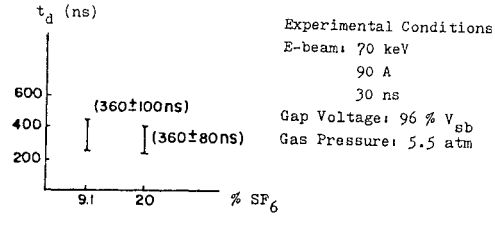

Fig. 8d. Delay Time vs % SF_6

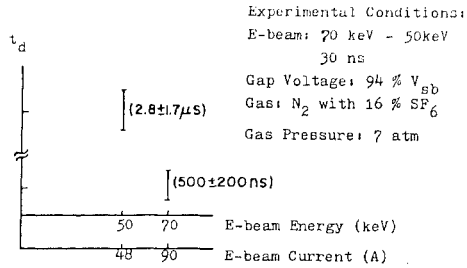

Fig. 8 e. Delay Time vs E-beam Current And Energy.

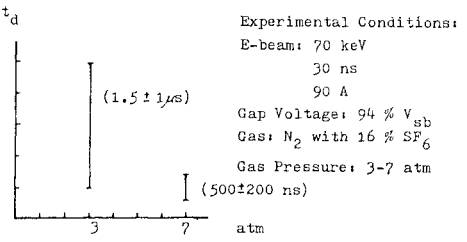

Fig. 8 f. Delay Time vs Gas Pressure.

Fig. 8. Delay Time vs E-beam and Gap Conditions.